



Indian Journal of Pure & Applied Physics
Vol. 58, August 2020, pp. 642-648



Enhancement in structural, morphological and optical features of thermally annealed zinc oxide nanofilm

Namrata Saxena^a, Varshali Sharma^b, Ritu Sharma^{a*}, K K Sharma^a, Kapil Kumar Jain^c, Santosh Chaudhary^d

^aDepartment of Electronics & Communication Engineering, Malaviya National Institute of Technology Jaipur, India

^bDepartment of Electrical & Computer Engineering, Carnegie Mellon University, Pittsburgh, USA

^cSolid State Physics Laboratory, DRDO, New Delhi, India

^dDepartment of Mathematics, Malaviya National Institute of Technology, Jaipur, India

Received 13 March 2020; accepted 6 July 2020

This paper presents the study of surface morphological, optical and microstructural features of zinc oxide (ZnO) nanofilm layered upon p-type Si substrate of <100> orientation by employing conventional RF magnetron sputtering system at different annealing temperatures. The effect of annealing on the nano-film is examined using different characterization techniques such as Atomic Force Microscopy (AFM), Scanning Electron Microscopy (SEM), X-ray Diffraction (XRD), FTIR (Fourier Transform Infrared Spectroscopy), UV-vis spectroscopy and Raman spectroscopy. The sharp diffraction peak at (002) orientation is seen by the XRD spectra which signifies a better growth of single crystalline thin film along the z-axis with the hexagonal wurtzite crystal structure. The surface morphological study shows that the grain size of the thin film intensifies from 22.06 nm to 36.77 nm when the annealing temperature is increased whereas there is a decrease in the values of lattice constants (a=b, c), FWHM (full width at half maximum), residual stress, lattice strain and dislocation density by increasing annealing temperature. The enhancement in the grain size makes the thin film appropriate for MEMS device applications including piezoelectric energy harvesters, gas sensors, etc. The optical bandgap of the ZnO thin film is estimated using Kubelka-Munk (KM) approach and it decreases from 3.23 to 3.16 eV for As-deposited, 400 °C, 600 °C and 800 °C respectively which makes the annealed thin film apposite for optoelectronic device applications. The intensity of the Raman peaks strengthens with the annealing temperature. These results prove that the annealing extensively enhances the crystallinity, structural, morphological and optical features of ZnO thin film and hence becomes suitable for nanoelectronic device applications.

Keywords: ZnO Thin Film, AFM, FTIR, Kubelka-Munk, Optical Bandgap, Raman Spectroscopy, SEM, Tauc-plot, UV-Vis, XRD.

Introduction

In the past few years, ZnO is materialized being a highly potential material for a wide variety of nanoelectronic, piezoelectric, piezoacoustic and optoelectronic device purposes. It offers higher exciton binding energy and the bandgap of 60 meV and 3.37 eV respectively. These features of ZnO makes it appropriate for numerous applications such as translucent electrodes in optoelectronics, in solar cells as TCO (Transparent Conducting Oxide), window and buffer layer, LEDs and LASERS, photodetectors (UV), heat mirrors in energy preservation and surface acoustic wave (SAW) devices. ZnO is utilized for MEMS (Micro Electro Mechanical System) and piezoelectric device

purposes because of its higher electromechanical coupling coefficient and large piezoelectric coefficient¹⁻⁵. The single crystalline ZnO nanostructures with z-axis orientation are essential for enhanced performance in several nanoelectronic device applications. During the last few decades, numerous techniques have been utilized for the deposition of ZnO thin film such as RF sputtering, thermal vapor deposition, sol-gel, e-beam deposition, pulsed laser deposition (PLD), molecular beam epitaxy (MBE), and metal organic chemical vapor deposition (MOCVD)¹⁻⁴. The quality of the ZnO thin film is reliant upon the film deposition techniques, type of substrate material and the growth conditions. A lot of experimentation has been done by the researchers to grow highly crystalline ZnO thin film deposited over silicon substrate because of its easy

* Corresponding author: (Email - rsharma.ece@mnit.ac.in)

availability of larger wafer sizes and reduced cost. The deposited ZnO film suffers from innate residual stress because of the variation in the large lattice mismatch between the silicon substrate and ZnO film and the thermal expansion coefficients. Thus, it is quite difficult to achieve the enhanced crystalline quality of the thin film deposited on the silicon substrate. Amongst the various deposition approaches RF magnetron sputtering is a much extensively employed method owing to its higher deposition rates, simpler set-up and lower substrate temperature. In the case of the RF sputtering technique, the characteristic features of the thin film depend on various parameters including RF Power, deposition time, temperature, pressure, and gas flow rate. RF sputtering is a comparatively appropriate technique employed for the deposition of ZnO thin film because of its numerous benefits such as easy control regulation for preferred crystalline orientation, epitaxial growth at comparatively low temperature, substantial packaging density, good surface adhesion along with the substrate^{1-4,6}.

This work focuses on the study of morphological, microstructural and optical features of thermally annealed zinc oxide nanofilm deposited over p-type <100> orientation silicon substrate using RF magnetron sputtering technique. To achieve the enhanced crystalline structure of the thin film annealing is performed by utilizing a conventional high-temperature tube furnace. To analyze the quality of the thin film, the microstructural, morphological and optical studies are performed using atomic force microscopy (AFM), X-ray Diffraction (XRD) and scanning electron microscopy (SEM) respectively. The optical features are studied by utilizing UV-Visible (NIR) spectroscopy, Raman spectroscopy and Fourier-transform infrared spectroscopy (FTIR).

2 Experimental details

ZnO Thin Film Deposition

The single-crystal ZnO thin film is deposited over p-type <100> orientation Si substrate (resistivity: 8-10 Ω cm and thickness \approx 380 μ m) using RF magnetron sputtering. The cleaning of the silicon wafer is performed by using acetone solution for the removal of dust particles and organic matter and afterward the sample is treated with HF dip for 5 min. (a solution of 1:9, 10% Hydrofluoric acid and 90% Water) for the removal of native SiO₂ (silicon

dioxide) from the silicon wafer. As it acts rapidly there is a necessity to expose the wafer just for a short time ("dip"). The thin film deposition is carried out using RF & DC magnetron sputtering (from Advanced Process Technologies, India) at room temperature by utilizing the ZnO target (3-inch dia target) containing 99% pure ZnO powder obtained from MERK Chemical Limited, Mumbai, India. In RF sputtering technique the vacuum for the deposition is generated at 6×10^{-6} mbar pressure at room temperature. Before the actual deposition, the process parameters are optimized to attain a better crystalline thin film. The deposition pressure and the deposition time are 6.8×10^{-3} mbar and 130 minutes respectively. The deposition rate varies in the range of 0.2 $\text{\AA}/\text{s}$ to 0.5 $\text{\AA}/\text{s}$ and the argon flow rate is maintained at 15 sccm throughout the deposition process.

ZnO Thin Film Annealing Process

After the deposition, the three different samples are then annealed at 400 $^{\circ}\text{C}$, 600 $^{\circ}\text{C}$, and 800 $^{\circ}\text{C}$ respectively, using high-temperature tube furnace (LTF 14/450) at the heating rate of 5 $^{\circ}\text{C}/\text{min}$. with the dwell time of 30 minutes, 22 minutes and 15 minutes respectively, to attain a better crystalline thin film. In this furnace, silicon carbide rod is used as the heating element. It has a high response rate as the heating element radiates heat directly onto the tube. For achieving maximum thermal efficiency and stability low thermal mass insulation is used throughout the worktube of the furnace.

ZnO Thin Film Characterization

The crystallographic properties are determined by X-ray Diffraction (XRD) (from PAN-alytical X'Pert - PRO) using Cu X-ray diffractometer controlled at 45 kV and 45 mA rating with Cu-K α radiation ($\lambda=1.5406\text{\AA}$) at the scanning rate of 0.02 $^{\circ}$ at 12 $^{\circ}$ min⁻¹ in the 2 θ range of 20 $^{\circ}$ to 70 $^{\circ}$. The structural investigation is performed by Atomic Force Microscopy (Multimode 8 Scanning Probe Microscope from Bruker Corporation, USA) in the tapping mode. The surface morphology is obtained using Field Emission Scanning Electron Microscope (from Nova Nano FE-SEM 450) carried out in high vacuum mode at 15 kV by employing Through Lens Detector (TLD). The Raman spectrum is detected through confocal micro Raman spectrometer (STR 500) through 532 nm excitation LASER,

12.5 mW LASER power, a $20\times$ objective lens, 45 second exposure and 600 G/mm. The UV-Vis spectroscopy is done using a UV-Visible spectrophotometer (Lambda 750 model from Perkin Elmer) with a 60mm diameter integrating sphere. The FTIR spectroscopy is studied using (spectrum two from Perkin Elmer) for achieving a plot between transmittance (%T) versus wavelength (cm^{-1}).

3 Results And Discussions

Analysis of Microstructural properties

The crystalline performance of the ZnO thin film is analyzed using XRD. The x-ray diffraction patterns of ZnO thin film annealed at three different temperatures 400 °C, 600 °C and 800 °C respectively. The thin film is identified as single crystalline in nature with the dominant peak of (0 0 2) orientation at $2\theta = 34.31^\circ$, 34.35° , 34.39° and 34.41° for as-deposited, 400 °C, 600 °C and 800 °C respectively is shown in Fig. 1. This single diffraction peak in XRD spectra ascribes to the superior quality of ZnO thin film along the z-axis. The grain size (D) is calculated using Debye Scherrer's^{1-2, 4-7} formula and it is noticed that the grain size increases from 22.06 nm to 36.77 nm from as-deposited to 800 °C sample, which makes this film appropriate for nanoelectronic device application⁴.

$$D = \frac{0.94\lambda}{\beta \cos\theta} \quad \dots (1)$$

where λ is the x-ray wavelength θ is the diffraction angle and β is Full Width Half Maximum(FWHM).

The assessment of the dominant diffraction peak with standard JCPDS card no. 00-036-1451⁸

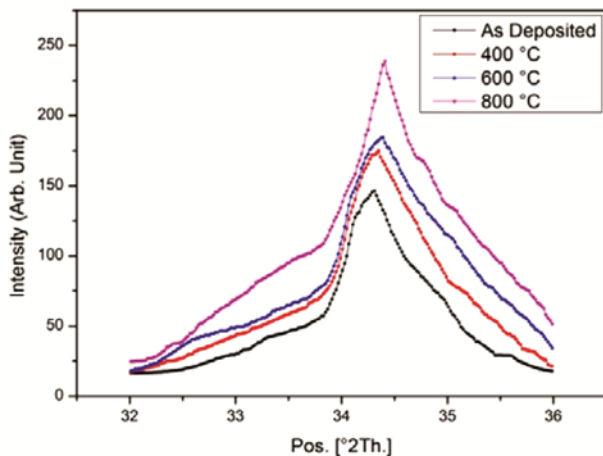


Fig. 1 — XRD pattern of ZnO thin film for $2\theta = 32^\circ$ to 36° at different annealing temperatures as-deposited, 400 °C, 600 °C and 800 °C.

implies that the ZnO thin film samples are crystalline in nature and it also confirms the hexagonal structure with space group (186) P63/mmc and wurtzite supergroup. The lattice parameters are calculated using Eq. (2) and Eq. (3) obtained from⁴. The calculated lattice values are in good agreement with the standard values ($a = b = 3.250\text{\AA}$, $c = 5.207\text{\AA}$) and crystal axial ratio as $c/a = 1.602$ obtained from JCPDS data. The dislocation density or the defect density provides considerable information regarding the crystal structure of the deposited thin film that can be expressed as the length of dislocations per unit volume which is given by Eq. (4) obtained from⁴.

$$a = b = \frac{\lambda}{\sqrt{3}\sin\theta} \quad \dots (2)$$

$$c = \frac{\lambda}{\sin\theta} \quad \dots (3)$$

$$\text{Dislocation Density} = \frac{1}{D^2} \quad \dots (4)$$

The lattice strain and the residual stress is computed using Eq. (5) and (6)

$$\text{Lattice Strain} = \frac{\beta}{4\tan\theta} \quad \dots (5)$$

$$\text{Residual Stress} = -233 \frac{(c-c_0)}{c_0} [\text{GPa}] \quad \dots (6)$$

where c_0 (5.206\AA) is the unstrained lattice constant for bulk ZnO⁴.

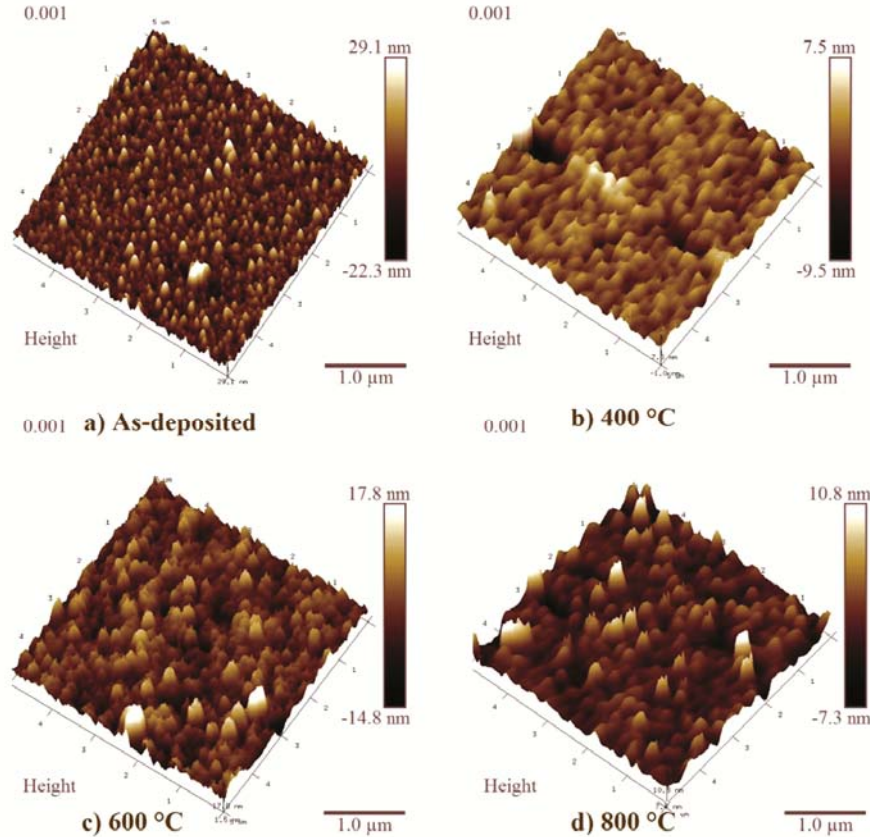
The negative value of the residual stress indicates that the compressive stress is developed in the thin film. There is an increment in the intensity of the dominant peak and the grain size in the XRD spectra. There is a decrement in the lattice constants, FWHM, dislocation density, lattice strain and residual stress with the increase in the annealing temperature enhancing the crystalline quality of the thin film. Many significant structural parameters like FWHM (β), grain size (D), the lattice constant, dislocation density, lattice strain, and residual stress are calculated and summarized in Table 1.

Analysis of Surface Morphological properties

Fig. 2. shows the $5 \times 5\ \mu\text{m}^2$ AFM images in 3-D view for as-deposited, 400 °C, 600 °C, and 800 °C respectively, each viewed at the scale of $1\ \mu\text{m}$. From these results, it is observed that the surface roughness

Table 1 — Effect of annealing on various significant microstructural parameters

Annealing temperature	2θ ($^\circ$)	β ($^\circ$)	D (Grain Size) nm	$a = b$ (\AA)	c (\AA)	Dislocation Density	Lattice Strain	Residual Stress
As-deposited	34.31	0.3936	22.06	3.015570944	5.223122089	2.0548×10^{-3}	3.18×10^{-1}	-0.766
400 $^\circ\text{C}$	34.35	0.3149	27.57	3.012164993	5.217222809	1.315×10^{-3}	2.59×10^{-1}	-0.502
600 $^\circ\text{C}$	34.39	0.2755	31.526	3.008767093	5.211337474	1.0061×10^{-3}	2.22×10^{-1}	-0.2388
800 $^\circ\text{C}$	34.41	0.2362	36.77	3.007071154	5.208400021	7.3962×10^{-3}	1.91×10^{-1}	-0.107

Fig. 2 — 3-D view of 200nm ZnO thin film at different annealing temperatures a) As-deposited, b) 400 $^\circ\text{C}$, c) 600 $^\circ\text{C}$ and d) 800 $^\circ\text{C}$

increases from 29.2 nm to 119 nm with an increase in the annealing temperature because of the increment in the grain size. This increment in roughness exhibits the same behaviour as reported in the literature⁹. The FESEM image of ZnO thinfilm at 200K \times magnification to describe the surface morphological variations with annealing temperature for as-deposited, 400 $^\circ\text{C}$, 600 $^\circ\text{C}$ and 800 $^\circ\text{C}$ respectively is shown in Fig. 3. From these images, it can be observed that the grown film is uniform and homogeneous in nature.

Analysis of Optical properties

For the calculation of optical bandgap, the reflectance is measured using a UV-Visible spectrophotometer with an integrating sphere of

60 mm diameter. The optical reflectance of the ZnO thin film is recorded in the range of 200 to 800 nm. The bandgap is calculated using Kubelka-Munk (KM or $F(R_{ef})$) method¹⁰ which is calculated using the following equation

$$F(R_{ef}) = \frac{(1-R_{ef})^2}{2R_{ef}} \quad \dots (7)$$

where $F(R_{ef})$ is proportional to the extinction coefficient (α), R_{ef} is the reflectance.

The photon energy (E) is calculated using the Brus formula as given by⁴

$$E = h\nu = \frac{1240}{\lambda} \text{ (eV)} \quad \dots (8)$$

where h is the Planck's constant in eV, λ is the wavelength in nm.

The $F(R_{ef})$ function is then multiplied with $h\nu$ to find the modified Kubelka-Munk function $(F(R_{ef})h\nu)$ and the bandgap E_g is calculated as follows¹⁰.

$$ah\nu \approx B(h\nu - E_g)^n \quad \dots (9)$$

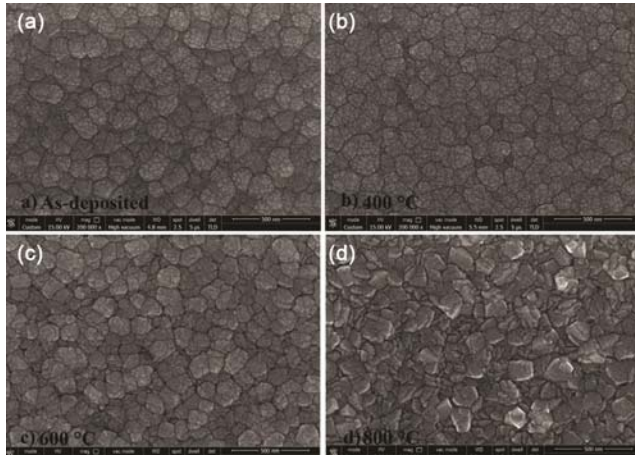


Fig. 3 — FESEM images of 200nm ZnO thin film at different annealing temperatures a) As-deposited, b) 400 °C, c) 600 °C and d) 800 °C

The Eq. (9) is modified as:

$$F(R_{ef})h\nu \approx B(h\nu - E_g)^n \quad \dots (10)$$

where B represents the absorption constant, n is the nature of band transition ($n = 1/2$ for the direct transition, $n = 3/2$ for the indirect transition) as reported in the literature^{4,10}. To plot the bandgap from the reflectance data $n = 1/2$ is substituted in Eq. (10). The graph amongst modified Kubelka-Munk function $(F(R_{ef})h\nu)^2$ and $h\nu$ is drawn. This graph is termed as the Tauc Plot¹⁰ and is shown in Fig. 4. The calculated bandgap (E_g) for the 200 nm ZnO thin film from the Tauc plot data is 3.23, 3.21, 3.18, 3.16 eV for the as-deposited, 400 °C, 600 °C and 800 °C respectively. The tendency of decrement of bandgap with the increment in the annealing temperature can also be validated by Varshni's empirical formula¹¹

$$E_g[T] = E_g[0] - \frac{\alpha T^2}{T+\beta} \quad \dots (11)$$

where $E_g[T]$ is the energy bandgap at temperature T , $E_g[0]$ is the bandgap at the 0 °K and α and β are constants.

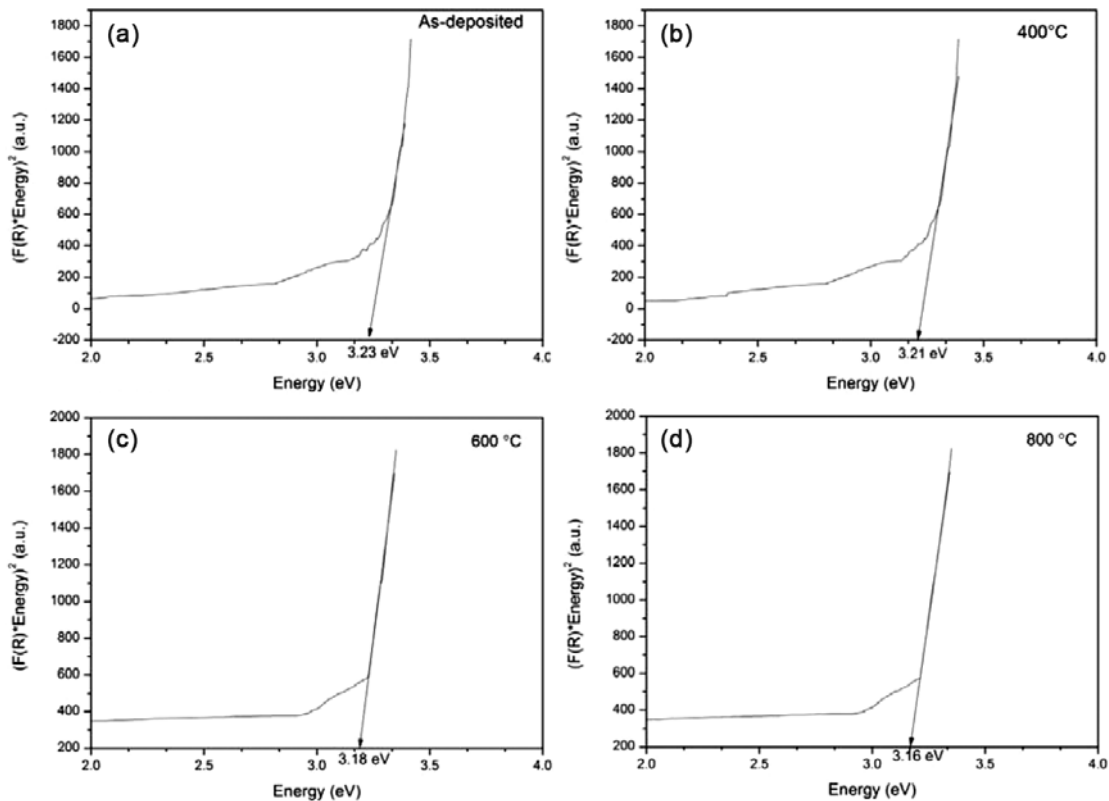


Fig. 4 — Tauc plot of ZnO thin film at different annealing temperatures. a) As-deposited, b) 400 °C, c) 600 °C and d) 800 °C

Fig. 5 shows the Raman spectra of 200 nm ZnO thin film ranging from 200 nm to 800 nm. The three Raman peaks of ZnO and the remaining two peaks of Si are obtained from the Raman spectra. The first ZnO peak occurs at $\sim 434 \text{ cm}^{-1}$ which indicates the presence of E2(High) vibrational mode of wurtzite ZnO structure. The shift from 437 cm^{-1} to 434.78 cm^{-1} of E2(High) is due to the lattice strain in the films^{2, 6, 12} which is in good agreement with the XRD result.

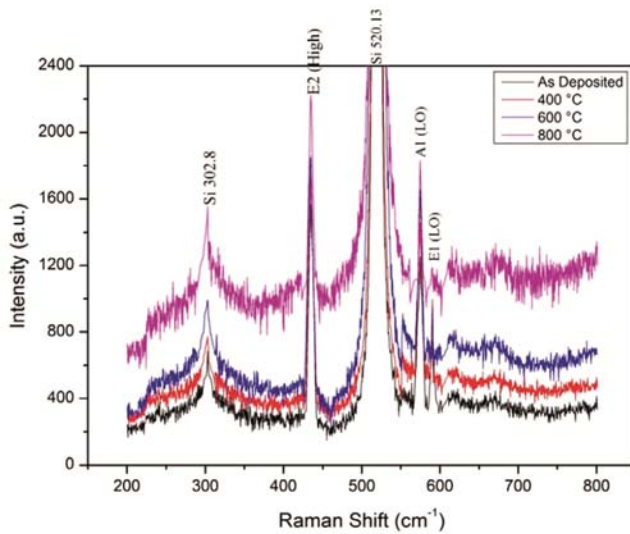


Fig. 5 — Raman Spectra of 200nm ZnO thin film at different annealing temperatures a) As-deposited, b) 400 °C, c) 600 °C and d) 800 °C

The higher intensity of the E2(High) vibration mode signifies the crystallinity improvement of the thin film^{2, 12-13}. The other two ZnO peaks appear at $\sim 574 \text{ cm}^{-1}$ and $\sim 583 \text{ cm}^{-1}$ which is associated with the A1 Longitudinal Optic (LO) and E1(LO) vibrations. The appearance of the peaks is in good agreement with the reported literature^{2, 12-13}. The intensity of the Raman peaks increases with the annealing temperature which leads to better crystalline thin film for optoelectronic and nanoelectronic device applications.

Fig. 6 demonstrates the transmittance (%T) as a function of wavenumber (cm^{-1}) of 200 nm ZnO thin film at different annealing temperatures. The minima in the transmittance spectra denote the maximum absorption corresponding to the typical molecules and groups in the range of 400 to 4000 cm^{-1} . These transmittance peaks marked in Fig. 6 depicts their bond strength. From the FTIR spectrum, the analysis of different metal-oxide bonds and functional groups is carried out. The vibrational bands from 400 to 550 cm^{-1} are associated with the characteristic stretching mode of the Zn—O bond. The aromatic rings appear around 700 to 800 cm^{-1} wavenumber. The absorption peak ranging from 1300-1000 cm^{-1} results from C—O stretching mode^{7, 14}. There is an additional maxima in 800 °C annealed film i.e., around 1400 cm^{-1} due to the existence of N=O bending^{7, 14}.

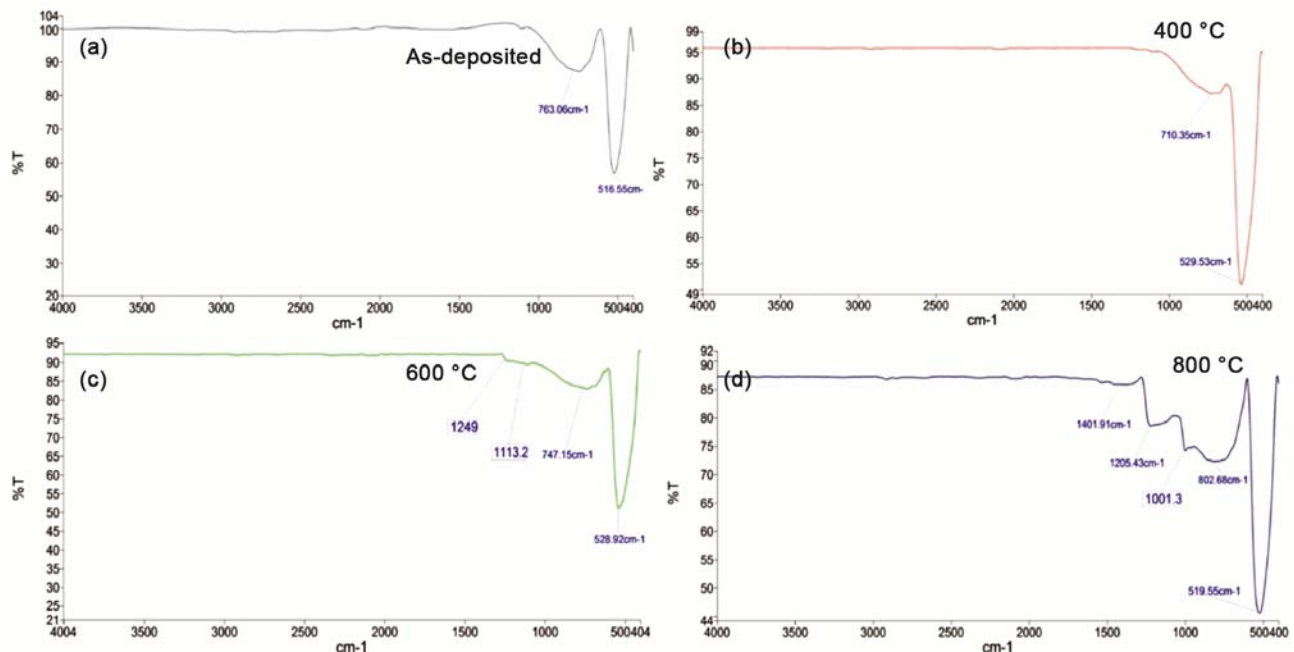


Fig. 6 — FTIR Spectra of 200nm ZnO thin film at different annealing temperatures a) As-deposited, b) 400 °C, c) 600 °C and d) 800 °C

CONCLUSION

In this paper the enhancement in structural, morphological and optical properties using thermal annealing of zinc oxide nanofilm is reported. When the as-deposited ZnO thinfilm is annealed at 400, 600 and 800 °C respectively the grain size intensifies from 22.06 to 36.77 nm with the decrement in the FWHM, dislocation density, lattice strain and residual stress. The optical bandgap decreases from 3.23 to 3.16 eV with the increase in annealing temperature making the thinfilm suitable for optoelectronic and nanoelectronic device applications.

ACKNOWLEDGEMENT

The authors wish to gratefully acknowledge DRDO, New Delhi for providing financial support to this project.

REFERENCES

- 1 Husna J, Aliyua M M, Islama M A & Chelvanathan P, *Energy Procedia*, 25 (2012) 55.
- 2 Sharma S, Bayer B C, Skakalova V & Singh G, *IEEE Trans Electron Dev*, 63 (2016) 1949.
- 3 Hazra P, Chakrabarti P & Jit S, *IOP Conf. Series: Materials Science and Engineering*, 73 (2015) 012092.
- 4 Sharma S, Vyas S, Periasamy C & Chakrabarti P, *Superlattices and Microstructures* 75 (2014) 378.
- 5 Hu S Y, Lee Y C , Lee J W & Huang J C, *Applied Surface Science*, 254 (2008) 1578.
- 6 Ismail A & Abdullah M J , *Journal of King Saud University – Science* (2013) 25 209.
- 7 Babu S K , Reddy A R., Sujatha Ch., Reddy K V & Mallika A N, *Journal of Advanced Ceramics*, 2 (2013) 260.
- 8 Cullity B D & Stock S R, *Elements of X-Ray Diffraction*, (Prentice-Hall, NY, USA), 3rd Edn. 2001.
- 9 Johari S, Muhammad N Y & Zakaria M R, *EPJ Web of Conferences*, 162 (2017) 01057.
- 10 Lopez R & Gomez R, *J Sol-Gel Sci Technol*, 61 (2012) 1.
- 11 Varshni Y P, *Physica*, 34 (1967) 149.
- 12 Dhara S & Giri P K, *Nanoscale Res Lett*, 6 (2011) 504.
- 13 Taziwa R, Ntozakhe L & Meyer E, *J Nanosci Nanotechnol Res*, 1 (2017) 1.
- 14 Xiong H M, Shchukin D G, Mhwald H, Xu Y & Xia Y, *Angew Chem Int Ed*, 48 (2009) 2727.